Assessment of 3D Shading Calculations for Photovoltaic System Modeling

Aron P. Dobos
Senior Engineer, NREL
aron.dobos@nrel.gov

Janine M. Freeman
Energy Modeling Engineer, NREL
janine.freeman@nrel.gov

Nicholas A. DiOrio
Modeling and Software Engineer, NREL
nicholas.diorio@nrel.gov

This paper assesses three popular models for estimating shading losses on photovoltaic systems. Several hypothetical and actual scenes are used to compare the loss predictions of the three dimensional (3D) shading calculators in the System Advisor Model (SAM), PVsyst, and PV*SOL tools. Comparisons with measured shade blocking from a SunEye device are also made for four actual systems. Results show some differences in hourly shade loss profiles among the studied tools, even for very simplistic geometries. However, on a monthly solar access basis, the differences appear to cancel out to some degree and result in errors that are comparable to documented variations in energy predictions. These outcomes suggest a need for further development and improvement of 3D shade calculators to reduce model prediction errors and inter-tool variability.

1 Introduction

Major reductions in the cost of photovoltaic (PV) systems in the past several years have led to a proliferation of PV deployments at all market scales. Particularly for distributed systems, which are frequently installed on existing rooftops in an urban environment, shading from nearby obstructions (other buildings, trees, etc) can have a major impact on energy production. However, as such losses in available irradiance may no longer banish a system from economic viability due to significant recent cost reductions, it becomes imperative to have accurate software tools to model shading losses in a 3D environment.

Several tools for shade impact assessment exist on the market. Common hardware include the SunEye [1] and SolarPathfinder [2] devices that require a site visit to the rooftop itself to take skydome blocking photographs that are subsequently processed by special software to estimate solar access at the proposed installation site. Reducing assessment, siting, permitting, and other so-called balance of system (BOS) costs often pushes solar vendors to try to minimize site visits and thus the need for accurate 3D modeling of shade loss becomes evident. Possible methods include Light Detection and Ranging (LiDAR) analysis [3], topographical assessment using geospatial information systems (GIS) [4], and of course 3D modeling in computer-aided design (CAD) software which is the subject of this present assessment.

Commonly used desktop software for photovoltaic system performance estimation include PVsyst [5], PV*SOL [6], and NREL's System Advisor Model (SAM) [7]. More recent additions to these offerings include Helioscope [8], PV Complete [9], and others. All of these tools estimate shading impacts by calculating the portion of a PV panel whose view of the sun is blocked by nearby obstructions at various times of the year. Each software includes an interactive user interface for laying out PV panels in 3D space, adding obstructions such as trees, telephone poles, angled roof segments, and other geometric features. Once the scene is defined, standard computer graphics techniques or ray tracing methods are used to determine the PV panel shade area fractions as the entire scene is transformed by rotation to mimic the movement of the sun over the horizon.

To date, published comparisons and validation of PV performance modeling tools has focused on energy production in well characterized systems without irregular obstruction shading [10,11,12,13,14]. In general, the collective data in these works indicate that most PV performance models, using typical assumptions for soiling and other losses, yield predictions within roughly ± 5 % of measured system performance. However, to date, the accuracy of 3D shading loss calculations has not been independently verified. In addition, one would expect shading loss predictions from all software tools to match very closely if not identically, as the linear shaded area calculations stem solely from geometric considerations. Furthermore, the sensitivity of estimated shade loss and impact on annual energy production to the accuracy of the 3D model itself remains unknown.

We investigate these issues using SAM, PVsyst, and PV*SOL to quantify and improve understanding of any dif-

ferences in modeled shade loss among the three tools, and provide a basis for further model improvement. This paper is organized as follows. First, the procedure in SAM for calculating 3D shading losses is presented as a representative example. Next, three extremely simple geometries are considered to quantify intermodel differences in shade loss profiles. Finally, we compare model predictions for four residential systems for which on-site shade measurements are available before wrapping up with some brief concluding remarks.

2 Assessment of Simple Geometries

The purpose of this investigation is to isolate and identify any differences in the geometrical calculations for shaded area performed by the three models considered in this paper. Three very simple but well-defined geometries were created in three locations to simultaneously test a selection of orientations, dimensions, and locations in the world. These scenes are shown in Fig. 1-3, with location information given in Table 1.

Location	Latitude	Longitude	Time zone
Denver, Colorado	39.73	-104.99	-7
Quito, Ecuador	-0.18	-78.46	-5
Perth, Australia	-31.95	115.85	8

Table 1. Locations of prototypical 3D geometries.

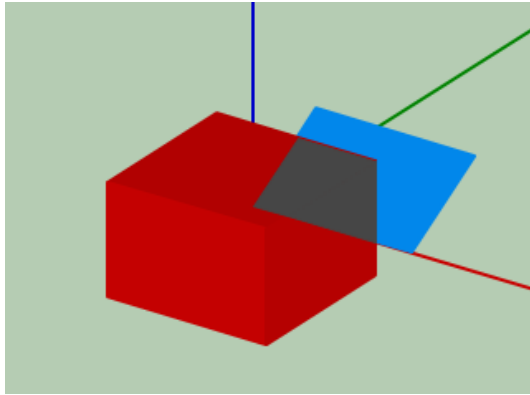

Fig. 1. Simple scene in Denver, Colorado.

After entering each scenario manually into SAM, PVsyst, and PV*SOL using each tool's interactive 3D scene editor, we exported simulation results and post processed them to extract the hourly beam irradiance shading loss. This data is readily provided by SAM's 3D shading calculator when used in the time series analysis mode. For PVsyst, the
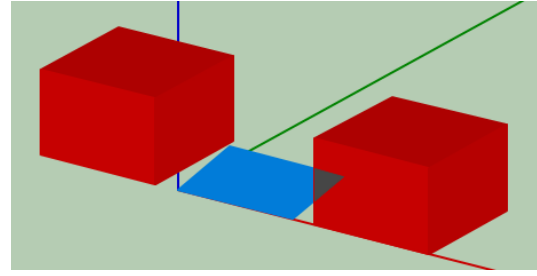

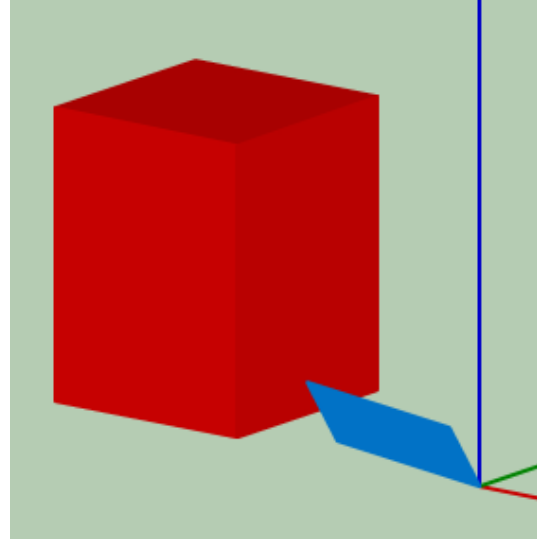
Fig. 2. Simple scene in Quito, Ecuador.

Fig. 3. Simple scene in Perth, Australia.

hourly data is given as a shade fraction from 0 (completely shaded) to 1 (unshaded) in the `FShdBm` data column.

Making a comparison with PV*SOL results is somewhat more complicated. PV*SOL does not directly provide a shaded fraction or similar output, and so the shading loss must be recovered from other data. Horizon shading effects that reduce the diffuse irradiance are first deducted from the total irradiance available to the modules, and this amount is then converted into a "rated" or nominal PV DC output. Then, the difference between nominal DC output power in kilowatt-hours and shaded DC output power in the same units can be used to recover an estimate for the beam shading fraction alone. First, we estimate the DC power loss from horizon shading L_h (kWh) at each our using the module's standard test condition (STC) efficiency:

$$L_h = L_{i,0} A \eta \tag{1}$$

where $L_{i,0}$ is the provided horizon irradiance loss in Watts/m^2, A is the module area, and η the STC efficiency. Then, the loss due to shadowing from obstructions may be retrieved at each hour:

$$L_s(\%) = 100 \cdot \frac{L_m + L_h}{M_0 + L_h} \tag{2}$$

where L_m is the reported module loss (kWh) and M_0 is the rated PV DC output. The horizon irradiance loss is added back into the rated PV DC output because PV*SOL derates the PV DC output by this loss before reporting the quantity.

Geometric shading loss for the three prototypical scenarios are shown in Fig. 4-6 for four representative days of the year. SAM and PVsyst estimate nearly identical shading losses but for some occasional deviations that are rather minor in magnitude at sun-up and sun-down hours for Denver and Quito. These deviations may result from small differences in the sun position calculation algorithms used by the tools, and the assumptions in each for how to handle hours in which the sun is only partially above the horizon. Although good agreement persists for Perth, PVsyst predicts a much more pronounced shade loss around hours 18-19 in January, April, and October than SAM, but only in that single hour of the day. One might presume that running these shade loss calculations at subhourly timesteps may recover finer detail of the actual shading profiles, which may explain some of these differences.

We also observe more frequent and more varied divergences in the PV*SOL's estimates of shading loss. Although the daily profiles agree fairly well in a qualitative sense for Denver, the Quito and Perth scenarios show significant differences. Differences seem to be greatest at the beginning and end of the day, and in some cases, such as on April 1st in Quito, over a 50 % absolute difference in shade loss for several hours in the day. PV*SOL shows better agreement with SAM and PVsyst before hour 15, after which it predicts much greater shading losses. The reasons for these differences are not immediately clear. Even if the post-processing procedure described previously is not perfect, one would expect differences in absolute magnitude but still a consistent shape to the loss profile. We would emphasize again, though, that in theory all three modules should predict identical geometric shading losses for these well-characterized prototypical scenarios.

In addition to beam irradiance shading losses arising from obstructions blocking the sun rays to the PV array, obstructions also reduce the effective portion of the sky dome visible to the array. Conservatively assuming an isotropic diffuse sky, the available diffuse irradiance is reduced by the view factor of the PV array to the sky, and remains constant through the year as the sun position does not affect the available sky diffuse. Estimated diffuse shading loss for the three scenarios are listed in Table. 2 for SAM and PVsyst. PV*SOL does not provide this value as an output.

SAM and PVsyst estimate similar diffuse loss in Quito and Perth, but PVsyst estimates more than twice the diffuse loss for the Denver scenario. The reason for this behavior is not clear and will require additional investigation.

3   Comparison with On-site Measurements

In this section, we apply the same procedures to four actual systems for which monthly solar access estimates have been measured using SunEye or SolarPathfinder devices. The system names and locations are listed in Table 3. This

Scene	SAM	PVsyst	PV*SOL
Denver	8.8 %	18.5 %	n/a
Quito	16.8 %	18.1 %	n/a
Perth	8.1 %	8.6 %	n/a

Table 2. Sky diffuse loss estimates for prototypical systems. PV*SOL does not provide this value as an output.

analysis does not purport to have the modeled 3D geometry of the roofs, trees, and PV systems impeccably reflect reality - but rather to be a "reasonable" model for each scene. Each scene was first entered into the SAM shading tool (Figs. 7-10, and then subsequently rebuilt in PVsyst and PV*SOL to as close an approximation as possible within the competence of the authors.

Name	City	Latitude	Longitude	Time zone
Ivanhoe	Denver	39.73	-104.98	-7
Babbitt	Los Angeles	34.24	-118.51	-8
Halsted	Los Angeles	34.24	-118.51	-8
Paradise	Soquel	36.99	-121.95	-8

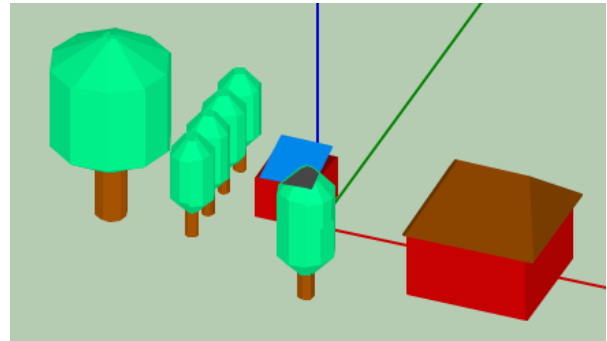Table 3.   Locations with on-site measurements.

Fig. 7.   Ivanhoe system in Denver, CO.

The estimated sky diffuse losses are listed in Table 4. We observe generally good agreement between SAM and PVsyst for all four systems.

Representative daily shading loss profiles for each system are shown in Figs. 11-14. In general, there is good qualitative agreement among all tools. SAM and PVsyst appear to be the closest to one another, while PV*SOL occasionally diverges significantly from the other tools, particularly at the begining or end of the day. For example, on October 1st, for the Ivanhoe system, PV*SOL predicts significantly
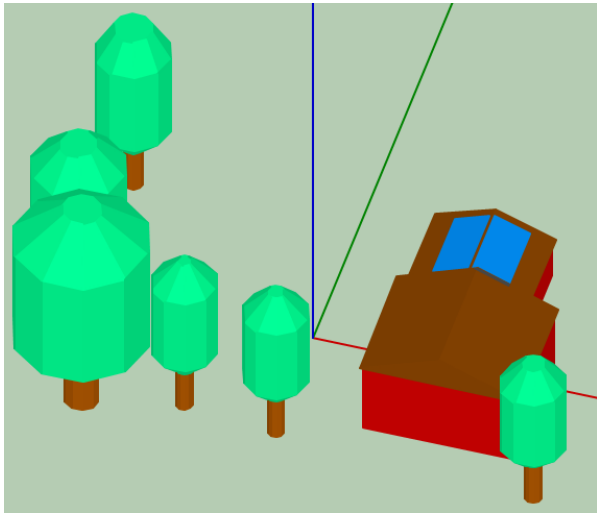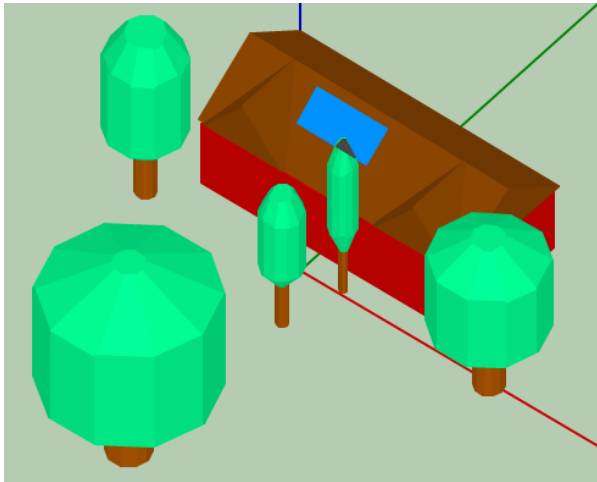
Fig. 8.   Babbitt system in Los Angeles, CA.
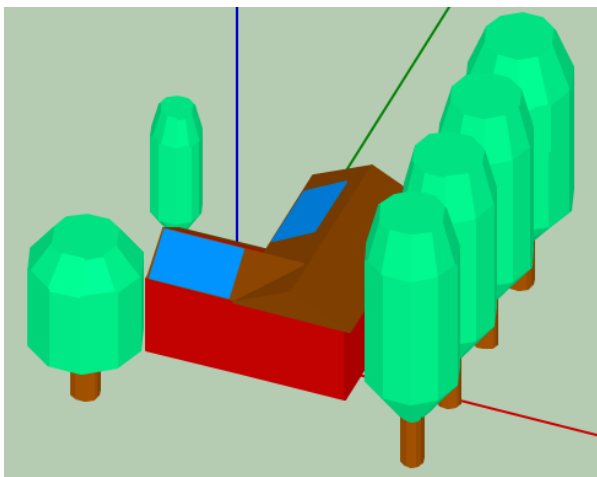

Fig. 9.   Halsted system in Los Angeles, CA.

Fig. 10.   Paradise system in Soquel, CA.

Scene	SAM	PVsyst	PV*SOL
Ivanhoe	17.7 %	20.7 %	n/a
Babbitt	9.3 %	7.3 %	n/a
Halsted	9.7 %	11.1 %	n/a
Paradise	12.4 %	12.1 %	n/a

Table 4.   Sky diffuse loss estimates for real systems. PV*SOL does not provide this value as an output.

lower shade losses in the afternoon after about 3 pm as the trees to the west obscure large portions of the array. Similar behavior can be observed for Paradise on January 1st, as generally among the other systems and times of the year.

Next, the calculated monthly solar access for each system is compared with measured estimates of monthly solar access from a SunEye or SolarPathfinder device in Table **??**. The values are plotted in Fig. 15, and show that all three tools match the site measurements adequately well, and general capture monthly loss trends. Fig. 16 shows the error relative to on-site measurements. Except for the Paradise system, all three tools are roughly within ±5 % on average of the on-site measurements. We stress however that the on-site measurements cannot necessarily be interpreted as the "truth" value, since there is likely not insignificant uncertainty in the sky photographing procedure as well as the subsequent image and data processing. Thus, the on-site measurement may well be considered to be just another modeled data point with an initial basis in the physical world.

4   Conclusions

This paper presents an assessment of 3D shading loss predictions from three popular PV modeling software packages, and compares their estimations with on-site measurements of solar access. Although there are some notable differences in predicted hourly beam irradiance shading losses, particularly at the beginning and end of the day, in general, all three models predict reasonably similar shade loss profiles. The same can be said of the monthly solar access predictions: for three of the four actual systems considered, all models compare within roughly ±5 % of on-side shade measurements. Thus, for annual energy yield estimation, 3D CAD modeling of obstruction shading for both beam and diffuse irradiance components can reasonably predict monthly and annual losses without direct rooftop measurement. That being the case, the demonstrated variability among tools should be investigated further so that the prediction errors can continue to be reduced for solar photovoltaic modeling approaches.

mensely grateful to Dr. T. T. Mai for sharing solar access measurements and system specifications for the "Paradise" system considered in this report.

References

[1] Solmetric SunEye 210 Shade Tool. `http://www.solmetric.com/buy210.html`, August 2016.

[2] Solar Pathfinder. `http://www.solarpathfinder.com`, August 2016.

[3] Jakubiec, J; Reinhart C.; *A method for predicting city-wide electricity gains from photovoltaic panels based on LiDAR and GIS data combined with hourly Daysim simulations*. Solar Energy, vol.93, pp.127-143, 2013.

[4] Melius J.; Margolis R.; Ong S.; *Estimating rooftop suitability for PV: a review of methods, patents, and validation techniques*. NREL TP/6A20-60593, 2013.

[5] PVsyst Version 6.47, `http://www.pvsyst.com`, August 2016.

[6] Valentin Software, PV*SOL Premium Version 2016 R6, `http://www.valentin-software.com/en/products/photovoltaics/57/pvsol-premium`, August 2016.

[7] National Renewable Energy Laboratory, *System Advisor Model*, `http://sam.nrel.gov`, August 2016.

[8] Folsom Labs, *Helioscope*, `https://helioscope.folsomlabs.com/`, August 2016.

[9] PV Complete, `http://pvcomplete.com`, August 2016.

[10] Blair, N.; Gilman, P.; Dobos, A. P. *Comparison of Photovoltaic models in the System Advisor Model*. American Solar Energy Society, SOLAR 2013 Conference, 2013.

[11] Freeman, J.; Whitmore, J.; Kaffine, L.; Blair, N.; Dobos, A.; *System Advisor Model: Flat Plate Photovoltaic Performance Modeling Validation Report*. NREL/TP-6A20-60204, 2013.

[12] Freeman, J.; Whitmore, J.; Blair, N.; Dobos, A.; *Validation of Multiple Tools for Flat Plate Photovoltaic Modeling Against Measured Data.* 2014 IEEE 40th Photovoltaic Specialist Conference (PVSC), Denver, CO, 2014.

[13] Haroon, S.; *PV Performance and Yield Comparisons, NREL SAM and PVSYST*. Suniva Corporation. Presentation at the SAM Virtual Conference, `https://sam.nrel.gov/conferences`, June 2012

[14] Yates, T., Hibberd, B., *Production Modeling for GridTied PV Systems*, Solar Pro Magazine, Issue 3.3, April/May 2010.
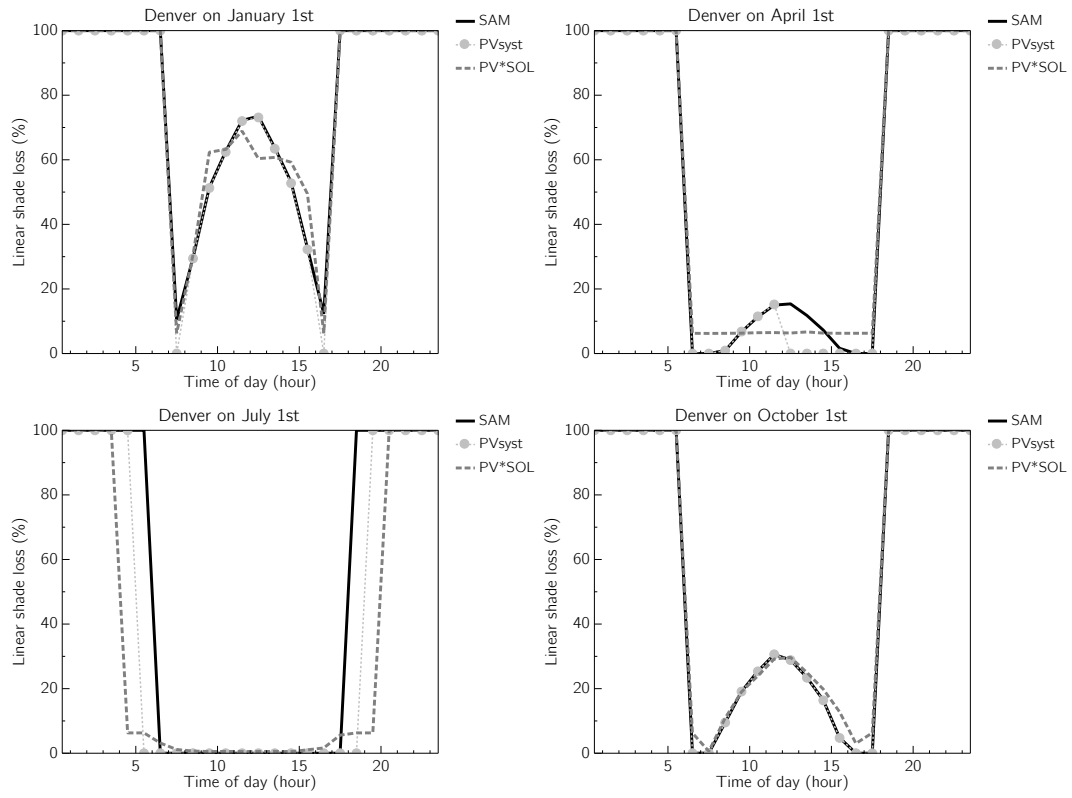
Fig. 4. Daily shade loss profiles for a prototypical system Denver, Colorado.
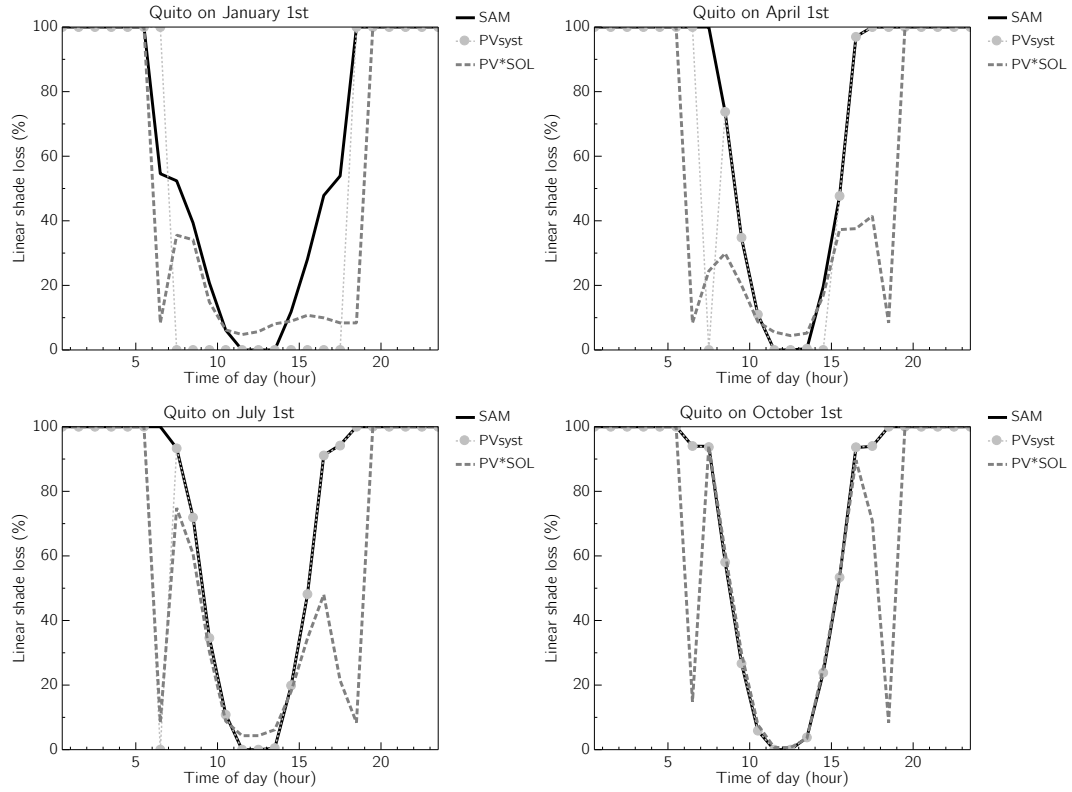
Fig. 5. Daily shade loss profiles for a prototypical system Quito, Ecuador.
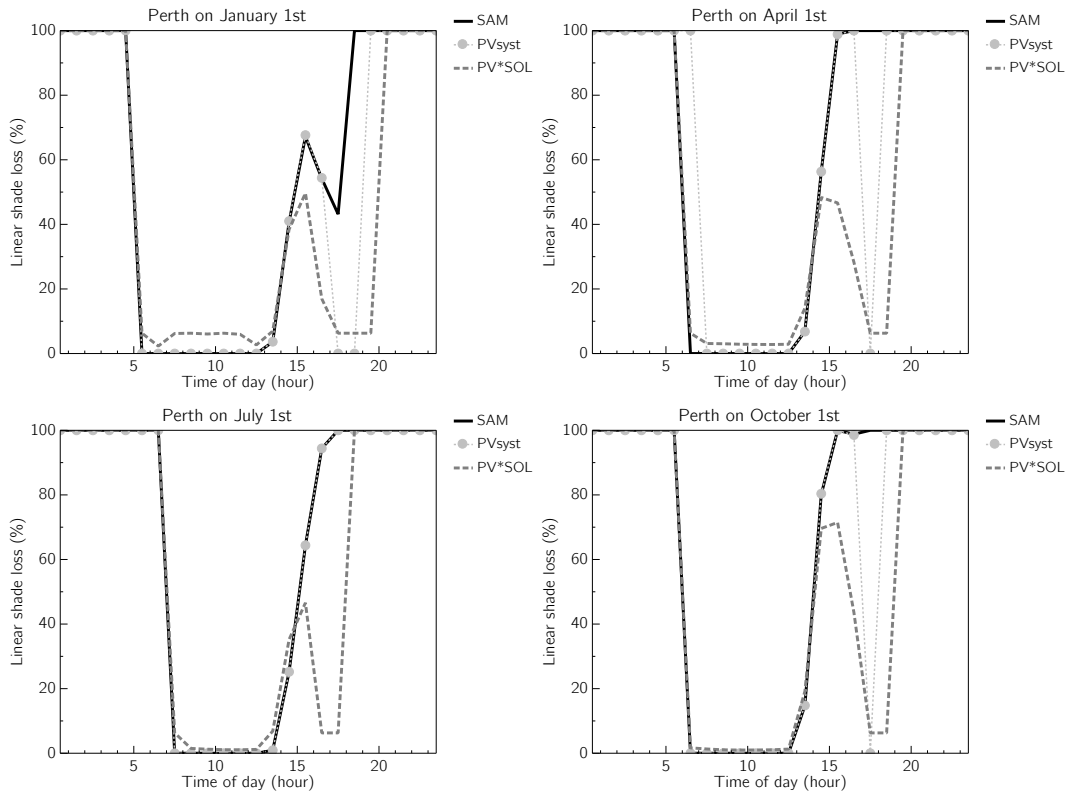
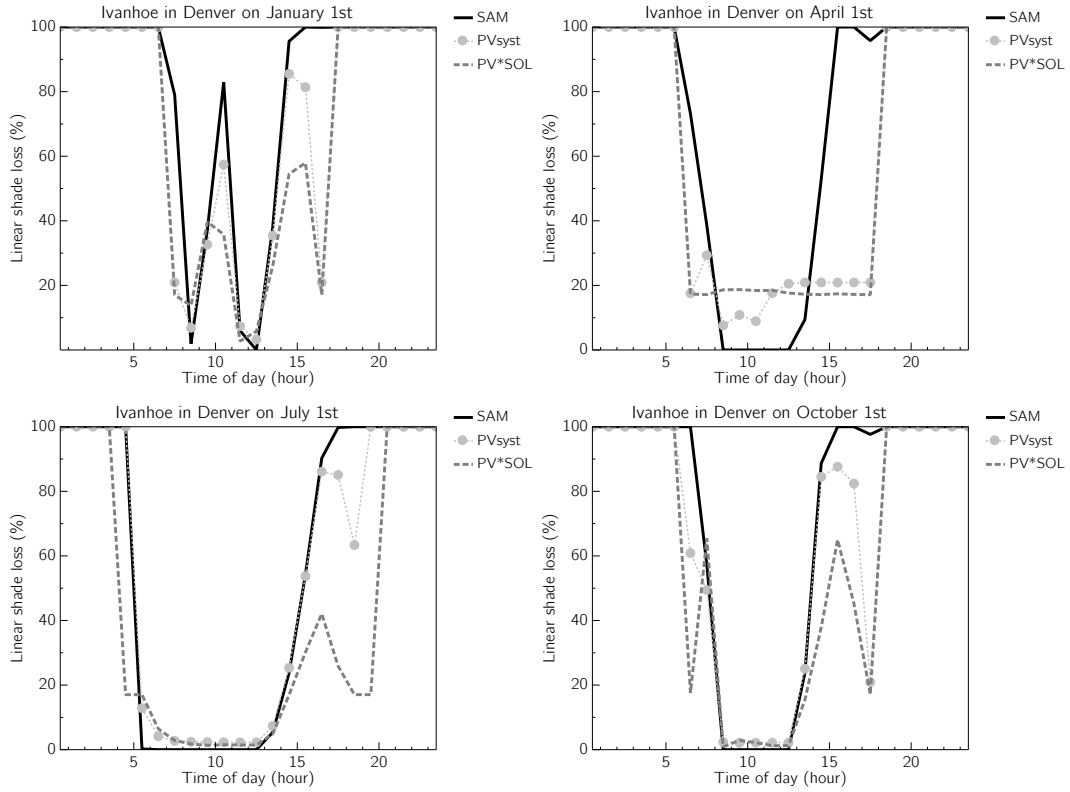Fig. 6.   Daily shade loss profiles for a prototypical system Perth, Australia.

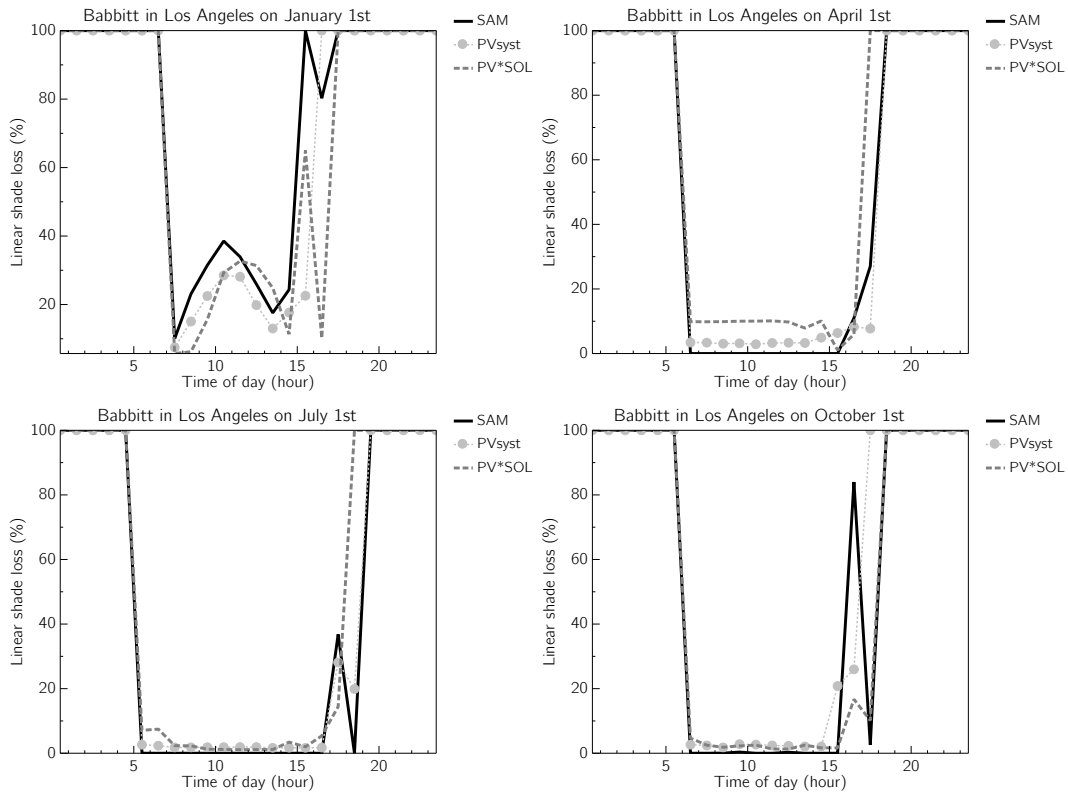Fig. 11.   Daily shade loss profiles for the Ivanhoe system in Denver.

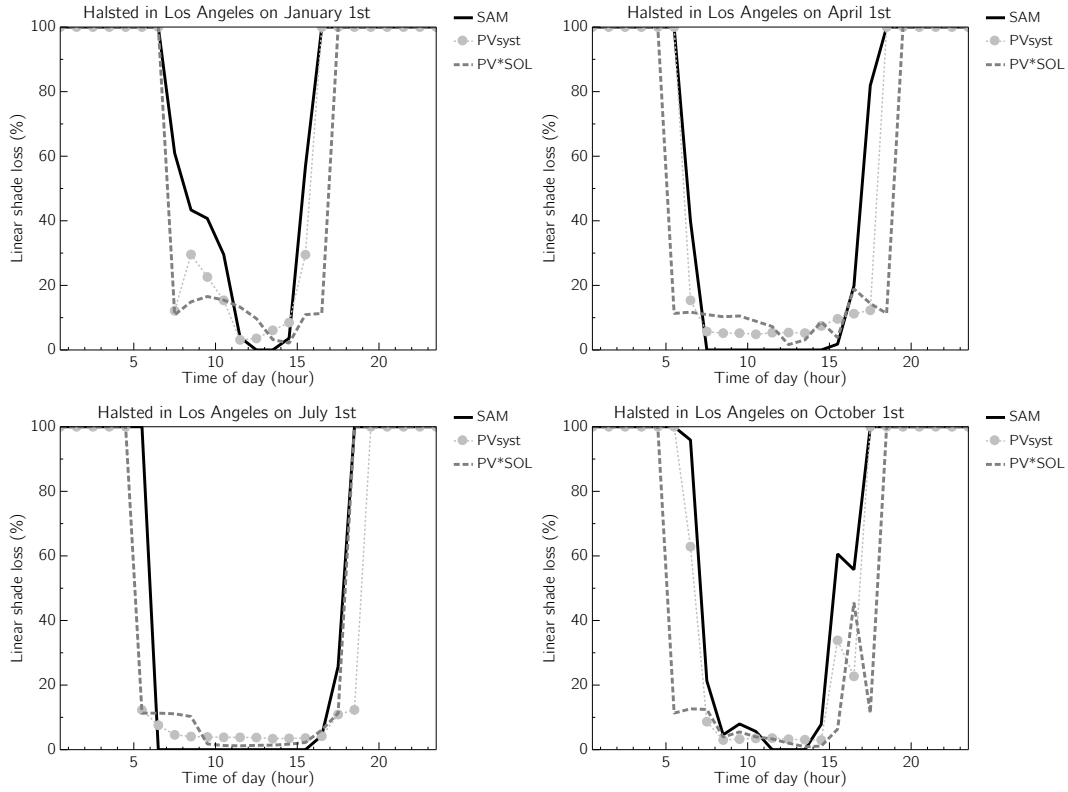Fig. 12. Daily shade loss profiles for the Babbitt system in Los Angeles.

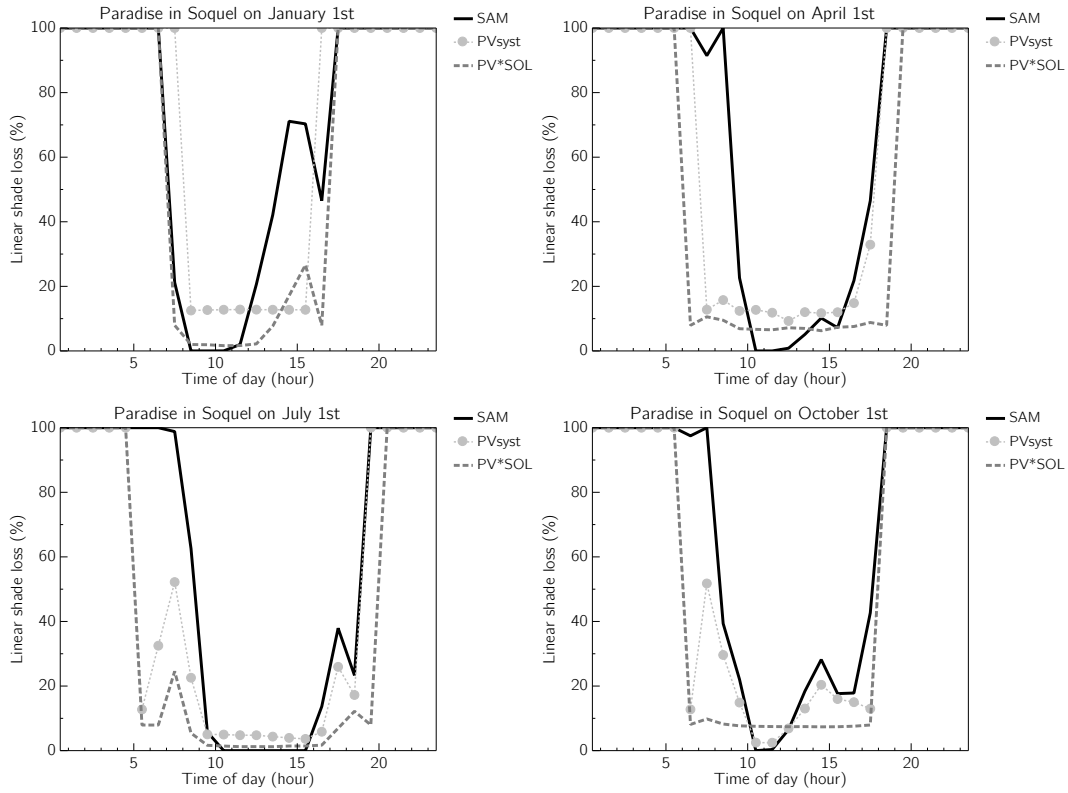Fig. 13. Daily shade loss profiles for the Halsted system in Los Angeles.

Fig. 14.   Daily shade loss profiles for the Paradise system in Soquel.

	Jan	Feb	Mar	Apr	May	Jun	Jul	Aug	Sep	Oct	Nov	Dec
Ivanhoe*	64	74	81	80	80	81	81	82	81	78	69	64
SAM	67	76	80	83	85	86	87	86	80	77	69	65
PVsyst	68	75	76	79	81	82	82	82	76	74	70	66
PV*SOL	75	77	79	82	85	86	86	85	78	77	74	75
Babbitt*	84	85	91	93	92	91	92	93	92	89	85	83
SAM	80	85	93	95	95	96	95	95	95	91	80	74
PVsyst	81	91	95	96	96	96	97	96	96	93	84	76
PV*SOL	80	88	95	96	94	96	96	96	95	92	84	79
Halsted*	83	86	91	94	95	95	96	96	91	89	84	81
SAM	84	84	92	96	96	96	96	96	95	87	83	84
PVsyst	86	87	92	95	94	94	95	95	94	90	86	86
PV*SOL	88	88	90	93	93	94	95	94	92	89	89	89
Paradise*	74	69	68	78	86	86	87	83	74	70	72	74
SAM	73	82	87	89	91	92	91	90	87	81	74	68
PVsyst	79	84	86	89	91	91	91	91	87	85	80	78
PV*SOL	92	94	93	93	93	94	94	94	92	93	93	92

Table 5.   Measured and modeled monthly solar access, in percent. '*' denotes measured value from a site survey using either a SunEye or SolarPathfinder device.
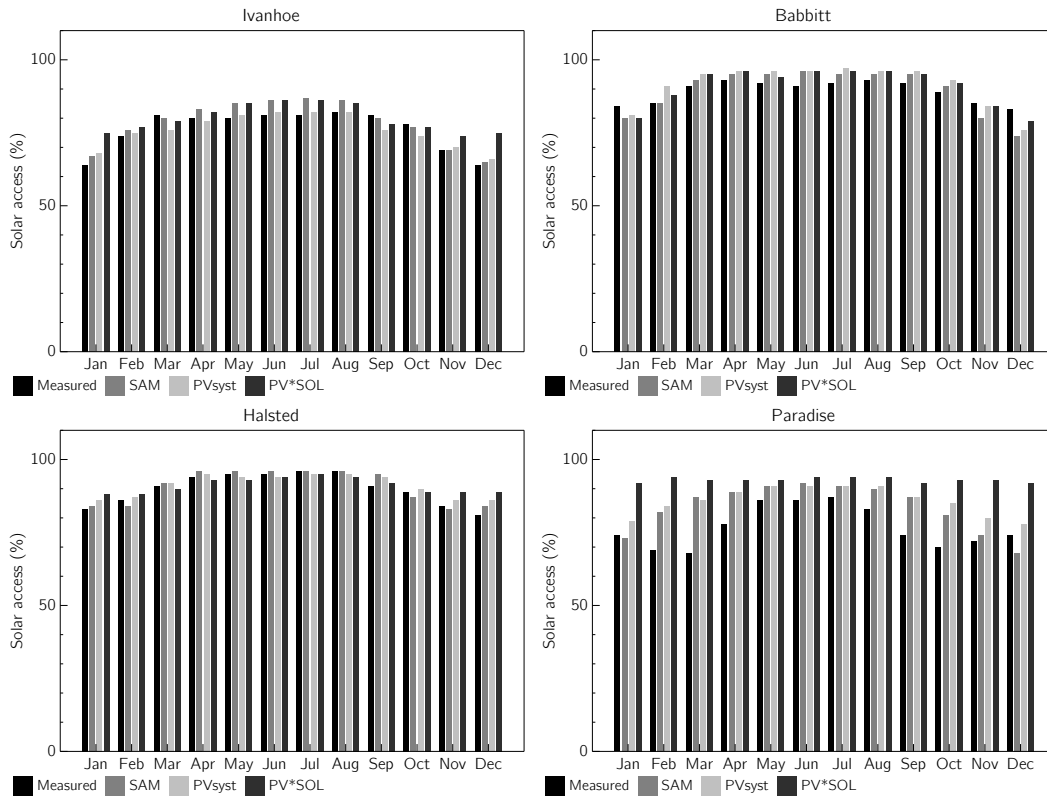
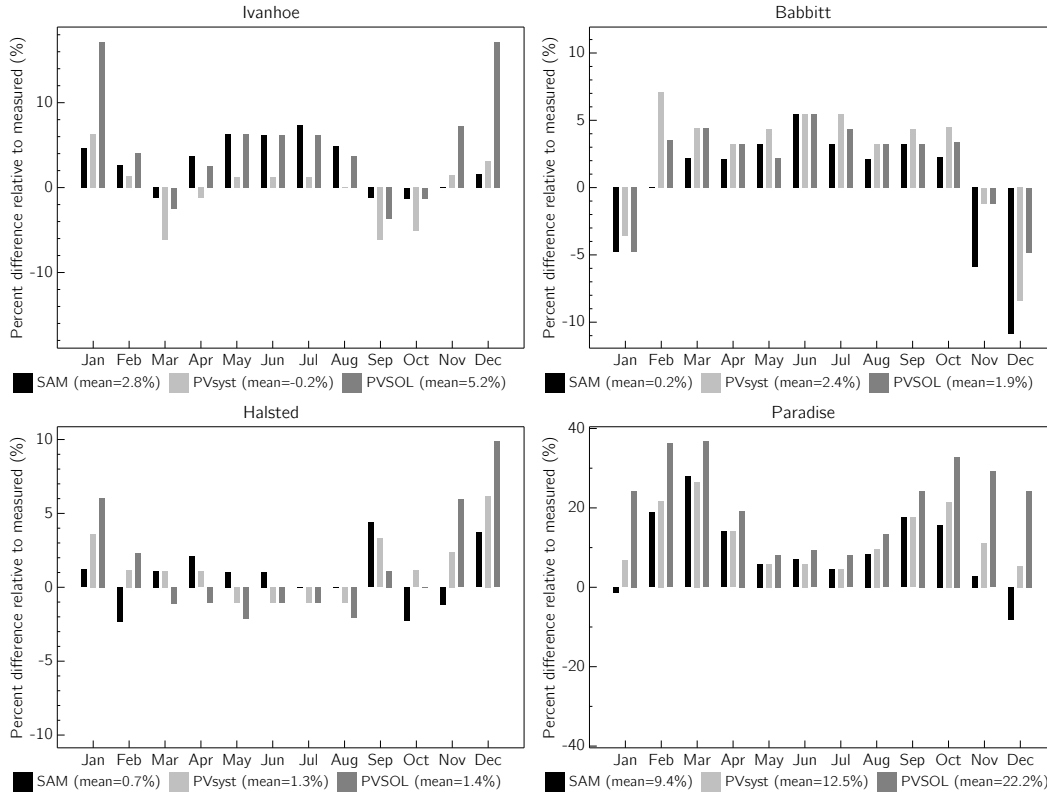Fig. 15.   Monthly solar access for four systems.

Fig. 16.   Difference in monthly solar access for four systems relative to SunEye or SolarPathfinder measurement.